ELSEVIER

Thin Solid Films 376 (2000) 183–187

thin solid films

www.elsevier.com/locate/tsf

Improvement of secondary electron emission property of MgO protective layer for an alternating current plasma display panel by addition of TiO_2

Rakhwan Kim, Younghyun Kim, Jong-Wan Park*

Department of Metallurgical Engineering, Hanyang University, Seoul 133-791, South Korea

Accepted 22 June 2000

Abstract

Secondary electron emission from a cathode material in an AC plasma display panel (PDP) is dominated by potential emission mechanism, which is sensitive to band structure of a protective layer. Therefore, the secondary electron emission property can be modified by a change in the energy band structure of the protective layer. $Mg_{2-2x}Ti_xO_2$ films were prepared by an e-beam evaporation method to be used as possible substitutes for the conventional MgO protective layer. The oxygen content in the films and in turn, the ratio of metal to oxygen gradually increased with increasing TiO_2 content in the starting materials. The stress relaxation, when the $[TiO_2/(MgO + TiO_2)]$ ratio in the evaporation starting materials was 0.15, seems to be related to the rough surface grown by Stranski–Krastanov mode due to the poor lattice matching condition between substrate and film. The film density, which was calculated from the refractive index, had a maximum at the $[TiO_2/(MgO + TiO_2)]$ ratio of 0.15 and then gradually decreased with a further increase in the $[TiO_2/(MgO + TiO_2)]$ ratio in the starting materials. When the $[TiO_2/(MgO + TiO_2)]$ ratios of 0.1 and 0.15 were used, the deposited films exhibited the secondary electron emission yields improved by 50% compared to that of the conventional MgO protective layer. © 2000 Elsevier Science S.A. All rights reserved.

Keywords: Alternating current plasma display panel; Protective layer; MgO–TiO_2 film; Secondary electron emission yield

1. Introduction

Color plasma display technology has been advancing quite rapidly in the area of large screen TV set since Fujitsu began the manufacture of the 42-inch full color alternating current plasma display panel (AC PDP) in 1995. Two key issues in order to meet the demands of advanced high vision PDP are production cost and power consumption, which are the stumbling blocks against the mass production of AC PDP [1]. Therefore, dramatic improvement of luminous efficiency and decrease in the power consumption are necessary and in turn, it is indispensable to optimize various component materials that can reduce the required voltage for discharging, and which will then be compatible with integrated circuits [2]. The operating voltage of AC PDP is largely affected by protective layer materials because the operation mechanism of AC PDP is based on the gas discharge phenomenon occurring around the protective layer that covers the dielectric layer [3].

There exists an excellent correlation between the firing voltage (V_f) and the secondary electron emission yield (γ) of protective layers in AC plasma display panels [4]. The higher the secondary electron emission yield of a protective layer, the lower the voltage of a panel can be obtained. Therefore, the development of the protective materials with higher secondary electron emission yield than MgO is essential for the improvement in overall electrical characteristics of AC PDP.

* Corresponding author. Tel.: +2-2290-0386; fax: +2-2298-2850.

0040-6090/00/$ - see front matter © 2000 Elsevier Science S.A. All rights reserved.
PII: S0040-6090(00)01184-6

The secondary electron emission property of the protective layer is affected by its energy band structure such as electron affinity, work function, bandgap energy and intraband level. In this work, in order to make a possible substitute for the conventional MgO protective layer, the effect of TiO_2 addition on the secondary electron emission characteristics of MgO protective layer were studied.

2. Experimental details

The evaporation sources were prepared using the solid-state reactions [5]. MgO and TiO_2 powders of 99.95% purity purchased from Cerac were used to prepare powder mixtures of desired compositions as a function of TiO_2 content in MgO. The powder mixtures were milled and then dry-pressed into disks in one direction at the pressure of 2000 Pa. Heat treatment at 1000°C were performed for 3 h in a vacuum furnace for densification of the cold-pressed mixture pellets. Each pellet with various TiO_2 content was deposited without elevating the substrate temperature and introducing oxygen gas into the evaporation chamber. Input power of electron gun and its high-voltage was fixed constant at 1.2 kW and 4 kV, respectively. The deposition time was adjusted to deposit films of appropriate thickness for analytical measurement. The substrate was p-Si(100) wafer which native oxide was removed by HF (hydrofluoric acid) treatment. Film stress was calculated from measured wafer curvature based on Stoney's equation using a Tencor FLX-2908 thin film stress measurement system [6]. The surface morphologies of the films were obtained by field emission scanning electron microscopy (FESEM). The chemical composition was determined by energy dispersive X-ray spectrometer (EDS) attached to FESEM. The refractive index of evaporated films was evaluated by AutoEL-II automatic ellipsometer and then the density was calculated by using the Lorentz–Lorenz relationship from measured refractive index [7].

The secondary electron emission properties of $Mg_{2-2x}Ti_xO_2$ films were characterized using the measurement system that was built at Seoul National University. The apparatus consists of an ion gun system, a measuring part for secondary electrons and a vacuum system, being similar to that of Lin et al. [8]. The detail description of the measurement system was already reported elsewhere [9]. Ion beams of He that are generated in the ion source are accelerated or decelerated to have constant kinetic energy. This ion beam strikes each sample and the secondary electrons emitted from the sample are collected by the collector part in accordance with the collector voltage. In this study, the He ion was chosen to be the ion species and its kinetic energy was fixed at 200 eV, because secondary electron emission from films depended upon the type and kinetic energy of ion species [10].

3. Results

Table 1 shows the chemical compositions and deposition rates of the films. As the $[TiO_2/(MgO + TiO_2)]$ ratio in the evaporation source materials increases, it is observed that a deviation from the linear relationship in Ti concentration between the starting materials and the deposited films appears. As the $[TiO_2/(MgO + TiO_2)]$ ratio in the starting materials increases up to 0.3, the cation ratio, $[Ti/(Mg + Ti)]$ in the films increases to 0.117. The deposited films are thus depleted to some degree in Ti concentration in comparison with the initial Ti composition in the starting materials. Besides it, the oxygen content in the films increases with increasing the TiO_2 content in the starting materials due to strong tendency of each titanium ion to combine with two oxygen ions as shown in Table 1. This increase in the oxygen content in the film leading to a change in its stoichiometry, i.e. the ratio of metal to oxygen $[(Mg + Ti): O]$, is believed to alter the energy band structure and then affect the secondary electron emission characteristics of protective layers [11]. The deposition rate of $Mg_{2-2x}Ti_xO_2$ films is in the range of 45–159 nm/min when the $[TiO_2/(MgO + TiO_2)]$ ratio in the starting materials varies from 0 to 0.3. The lower Ti concentration than that of the evaporation starting materials and decrease in deposition rate with addition of TiO_2 to MgO are well anticipated since these are indeed closely related to the vapor pressure of TiO_2 lower than that of MgO [12].

Table 1
Composition and deposition rate of $Mg_{2-x}Ti_xO_{2x}$ films

$[TiO_2/(MgO + TiO_2)]$ in starting materials	Cation ratio $[Ti/(Mg + Ti)]$	Metal to oxygen ratio $[(Mg + Ti):O]$	Deposition rate (nm/min)
0	0	1:1.02	159
0.05	0.026	1:1.16	120
0.1	0.054	1:1.19	105
0.15	0.069	1:1.19	96
0.2	0.092	1:1.20	63
0.3	0.117	1:1.23	45

The dependence of residual stress of $Mg_{2-2x}Ti_xO_2$ films of 5000 Å in thickness on the $[TiO_2/(Mg+TiO_2)]$ ratio in the starting materials is shown in Fig. 1. Thermal stress contribution to the measured stress is thought to be negligible because substrates were not heated during evaporation. The MgO film without addition of TiO_2 shows a little compressive stress of approximately 350 MPa. An increase in the TiO_2 content leads to increase in the compressive stress of $Mg_{2-2x}Ti_xO_2$ films and the stress of the film with $x=0.1$ in the starting materials is the largest. It is apparently expected from the fact that the ionic radii of Ti and O are larger than that of Mg. When the ratio becomes larger than 0.1, the compressive stress, however, gets relaxed remarkably. The relaxation of the compressive stress, when x is larger than 0.1 in the starting materials, is thought to be induced by rough surface of the films grown by Stranski–Krastanov growth mode due to poor lattice matching with Si substrate [13].

The surface morphologies of 5000-Å thick $Mg_{2-2x}Ti_xO_2$ films analyzed by FESEM are shown in Fig. 2. The surface morphology of the film with x of 0.1 (Fig. 2b) is very fine and uniform compared to that of the pure MgO film (Fig. 2a). It is shown that a film with a proper composition can be very uniformly deposited by e-beam evaporation and in turn, this might help improve the voltage stability of a panel in long time operations. However, an excessive addition of TiO_2 to MgO, such as the case when the $[TiO_2/(MgO+TiO_2)]$ ratio in the starting materials is as high as 0.2 or 0.3 (Fig. 2c,d), tends to make film surface rough as mentioned above, and furthermore initiate crack as shown in Fig. 2d. These cracks may also lead to instability in electron emission from the film surface and furthermore, reduce the lifetime of PDP because the dielectric layers cannot be effectively protected during long time operation.

Fig. 3 shows the surface roughness of $Mg_{2-2x}Ti_xO_2$ films as a function of $[TiO_2/(MgO+TiO_2)]$ ratio in the starting materials. When the $[TiO_2/(MgO+TiO_2)]$ ratio is 0.1, the deposited film has the lowest surface roughness. When the ratio is further increased, the

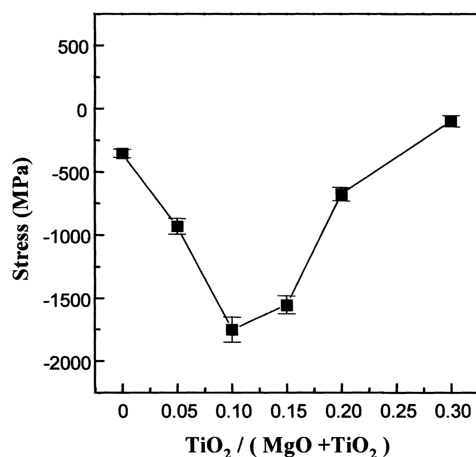

Fig. 1. Residual stress of $Mg_{2-2x}Ti_xO_2$ thin films as a function of $[TiO_2/(MgO+TiO_2)]$ ratio in the starting materials.

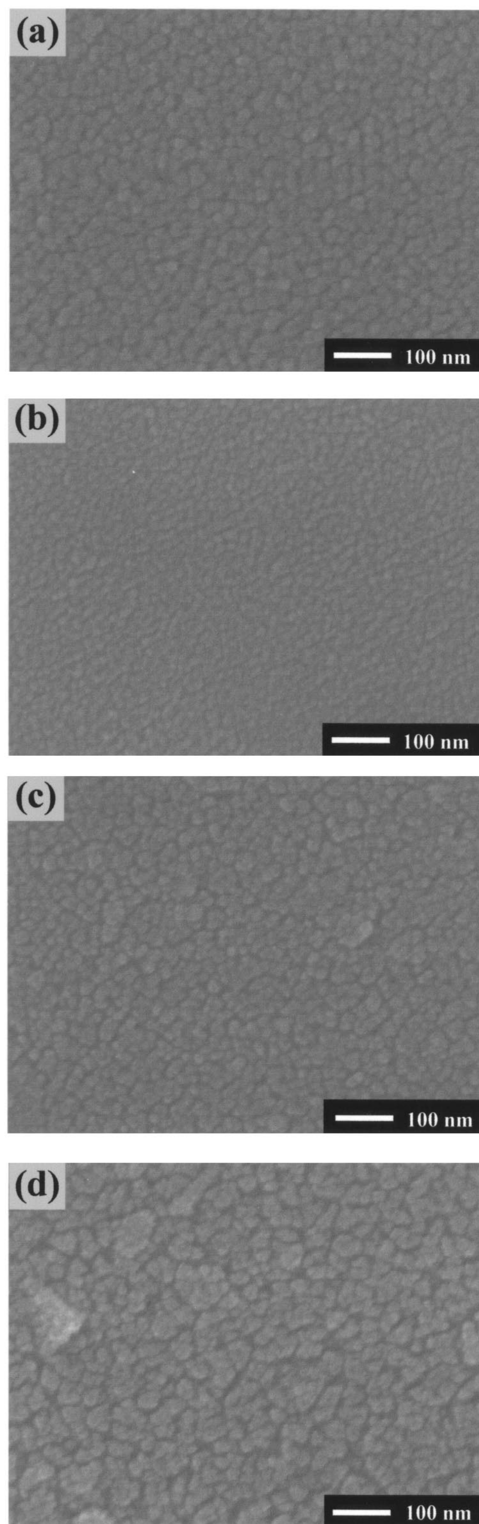

Fig. 2. FESEM images of $Mg_{2-2x}Ti_xO_2$ thin films as a function of $[TiO_2/(MgO+TiO_2)]$ ratio in the starting materials: (a) 0; (b) 0.1; (c) 0.2; and (d) 0.3.

film, however, shows an increase in the surface roughness due to Stranski–Krastanov growth. Fig. 4 shows the refractive index analyzed by the measurement of ellipsometry as a function of TiO_2 content in the starting materials. The refractive index of the bulk MgO is 1.736 but that of evaporated MgO films is 1.634 ± 0.01, much smaller than that of bulk MgO due to the fact that thin films generally contain many micropores which reduce film density. The refractive index of the films gradually increases to 1.735 with increasing TiO_2 content in the starting materials to 0.15 followed by a slight decrease and saturation above TiO_2 content of 0.15. The density of films can be calculated from refractive index by Lorentz–Lorenz equation,

$$\rho = K(n^2 - 1)/(n^2 + 2) \tag{1}$$

where ρ, K, and n are film density, a constant and measured refractive index, respectively. The K value is 9.078, which is calculated from the refractive index (1.737) and the density (3.65 g/cm^3) of the bulk MgO. The density of pure MgO film is 3.224 g/cm^3, which is 89% of bulk MgO density. The film density has a maximum at the $[TiO_2/(MgO + TiO_2)]$ ratio of 0.15 and gradually decreases with increasing the $[TiO_2/(MgO + TiO_2)]$ ratio, exhibiting a similar behavior to the refractive index.

Fig. 5 shows the measured target (I_T) and collector (I_C) currents as a function of the collector bias voltage (V_C) relative to the target when 200 eV He^+ beam is bombarding on the film with the $[TiO_2/(MgO + TiO_2)]$ ratio in the starting materials of 0.20 deposited on p-type Si wafers. When the collector voltage is smaller than zero, target current is the same as the ion beam current. When it increases above zero, the target current comprises a film current (ion beam current) and a current by the secondary electron emission from a film. The secondary electrons are collected at the collector part. Therefore, secondary electron emission yield, which is defined as the number of emitted secondary electrons over the number of incident ions, can be calculated by Eq. (2).

$$\text{Secondary electron emission yield } (\gamma) = (I_{T[V_c > 0]} - I_{T[V_c < 0]})/I_{T[V_c < 0]} \tag{2}$$

Low operation voltage is needed to reduce the cost of driving ICs, which can be obtained by increasing the secondary electron emission yield of a cathode material since the firing voltage is dependent on γ. Thus, it is desirable to measure the secondary electron emission yield of $Mg_{2-2x}Ti_xO_2$ films as a function of TiO_2 content in the starting materials. Fig. 6 shows the measured secondary electron emission yield of each film. Despite a small variation in Ti cation ratio from 0 to 0.092 in film, the corresponding change in the secondary electron emission coefficient turned out to be very large. The secondary electron emission yield of the

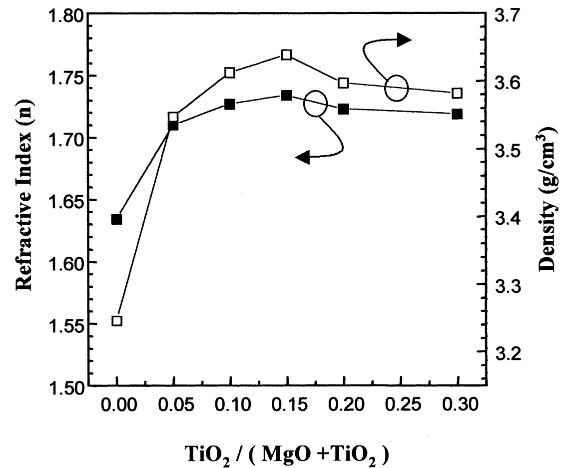

Fig. 4. Refractive index and film density of $Mg_{2-2x}Ti_xO_2$ films as a function of $[TiO_2/(MgO + TiO_2)]$ ratio in the starting materials.

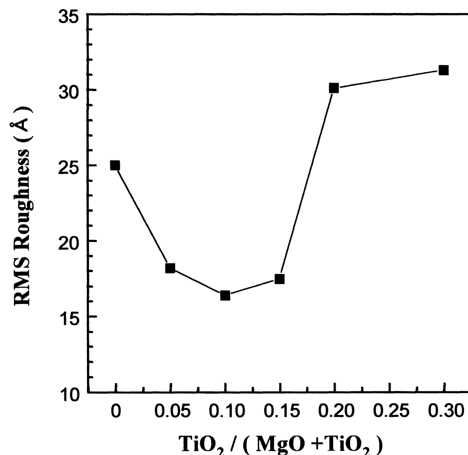

Fig. 3. Surface roughness of $Mg_{2-2x}Ti_xO_2$ films as a function of $[TiO_2/(MgO + TiO_2)]$ ratio in the starting materials.

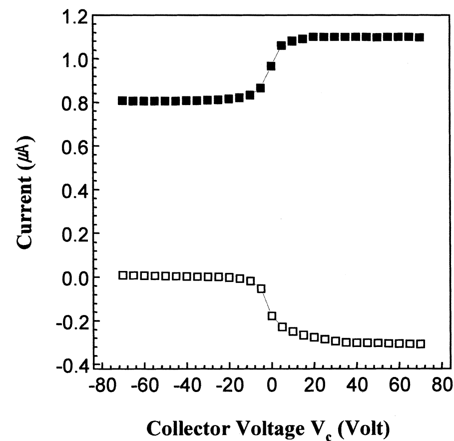

Fig. 5. Measured current I_T (filled rectangular) and I_C (open rectangular) for the film with the $[TiO_2/(MgO + TiO_2)]$ ratio of 0.20 as a function of the collector voltage V_C.

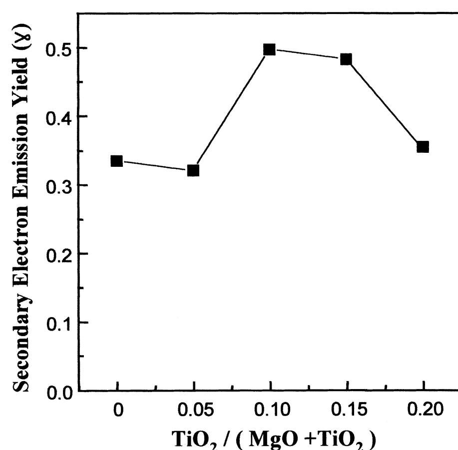

Fig. 6. Secondary electron emission yields of $Mg_{2-2x}Ti_xO_2$ films as a function of $[TiO_2/(MgO+TiO_2)]$ ratio in the starting materials

pure MgO film is 0.33. The films with the $[TiO_2/(MgO+TiO_2)]$ ratio in the starting materials of 0.1 and 0.15 (cation ratio of 0.054 and 0.069) exhibit the secondary electron emission yield of about 0.495 and 0.482, respectively. When the $[TiO_2/(MgO+TiO_2)]$ ratio is 0.2, the yield is, however, decreased to 0.349. Electrical instability was observed when the ratio was 0.3. This instability is probably due to the crack, as shown in Fig. 2d, which made the measurement of the secondary electron emission yield unsuccessful.

From these results, it can be inferred that the secondary electron emission property of the $Mg_{2-2x}Ti_xO_2$ films can be greatly improved by addition of a proper amount of TiO_2 to MgO. The band gap energies of MgO and TiO_2 are 7.3 and 3.7 eV, respectively [12]. It is suggested that a change in the energy band structure such as excess oxygen band is one of the main reasons for enhancement in the secondary electron emission property of $Mg_{2-2x}Ti_xO_2$ film. Once oxygen content in films reaches a critical point (above the $[TiO_2/(MgO+TiO_2)]$ ratio in the starting materials of 0.15), the proportionate relationship between excess oxygen band and the secondary electron emission characteristics is no longer effective. This is probably due to the poor film morphology mentioned above, which is consistent with the appearance of the inflection points in the film stress and the surface roughness as shown in Figs. 1 and 3, respectively. Furthermore, the variation in the film density also somewhat supports the phenomenon that the secondary electron emission is affected by TiO_2 addition to MgO. However, it needs further in-depth study to understand which properties of TiO_2 really affect the MgO-base emission characteristics of the protective films.

4. Conclusion

$Mg_{2-2x}Ti_xO_2$ films were prepared by an e-beam evaporation method to be used as a possible substitute for the conventional MgO surface protective layer for dielectric materials in AC PDPs. When the $[TiO_2/(MgO+TiO_2)]$ ratio in the starting materials was increased up to 0.3, the cation ratio in the film increased to 0.117 and the oxygen content in the films gradually increased. The relaxation of the compressive stress of the films, when the $[TiO_2/(MgO+TiO_2)]$ ratio in the starting materials is 0.2, seems to occur due to rough surface of the films. The density of pure MgO film was 3.224 g/cm^3, which is 89% of bulk MgO density. The film density had a maximum at the $[TiO_2/(MgO+TiO_2)]$ ratio of 0.15 and gradually decreased with further increase in the $[TiO_2/(MgO+TiO_2)]$ ratio. The $Mg_{2-2x}Ti_xO_2$ films yielded a secondary electron emission coefficient as high as 0.497 when the $[TiO_2/(MgO+TiO_2)]$ ratio in the starting materials was 0.1, while the secondary electron emission yield from a pure MgO film was 0.33. Such increase in the secondary electron emission yield is expected to lead to a great improvement in the voltage characteristics of panels.

Acknowledgements

The authors would like to thank the PDP Research Division (G7 project) in Korea for financial support and Professor Jihwa Lee at Seoul National University for his technical support on the measurement of secondary electron emission yield.

References

[1] S. Mikoshiba, Society for Information Display 15 (2/1999) 28.
[2] T. Shinoda, H. Uchiike, S. Andoh, IEEE Trans. Electron Devices 26 (1979) 1163.
[3] T. Urade, T. Imemori, M. Osawa, N. Nakayama, I. Morita, IEEE Trans. Electron Devices 23 (1976) 313.
[4] A. Shiokawa, Y. Takada, R. Murai, H. Tanaka (Eds.), Kobe, Japan, December 7-9, 1998, Proceedings of International Display Workshops 98 (1998) 519.
[5] J. Cho, R. Kim, K.-W. Lee, G.-Y. Yeom, J.-Y. Kim, J.-W. Park, Thin Solid Films 350 (1999) 173.
[6] J. Cho, R. Kim, K.-W. Lee, G.-Y. Yeom, J.-Y. Kim and J.-W. Park, Thin Solid Films (accepted).
[7] D.E. Aspnes, Thin Solid Films 89 (1982) 249.
[8] H. Lin, Y. Harano, H. Uchiike, ASID Technical Digest (1995) 70.
[9] K.S. Moon, J.W. Cho, J. Lee, K.-W. Whang, Seoul, Korea, Sept. 28-Oct. 1, 1998, Proceedings of The 18th IDRC/ISSN-0098-966X (1998) 401.
[10] A. Shiokawa, Y. Takada, R. Murai, H. Tanaka, Seoul, Korea, Sept. 28-Oct. 1, 1998, Proceedings of The 18th IDRC/ISSN-0098-966X (1998) 519.
[11] Y. Ushio, N. Matuda, S. Bana, A. Kinbara, Thin Solid Films 167 (1988) 299.
[12] G.V. Samsonov, The Oxide Handbook 2nd edition, IFI/Plenum Data Corporation, New York, 1982, p.144.
[13] Milton Ohring, The Materials Science of Thin Films, Academic Press, Boston, 1992, p.197.